Adsorption Equilibrium of Methane, Carbon Dioxide, and Nitrogen on Zeolite 13X at High Pressures

Simone Cavenati, Carlos A. Grande, and Alírio E. Rodrigues*

Laboratory of Separation and Reaction Engineering, Department of Chemical Engineering, Faculty of Engineering, University of Porto, Rua Dr. Roberto Frias s/n, 4200-465, Porto, Portugal

High-pressure adsorption of methane, carbon dioxide, and nitrogen on zeolite 13X was measured in the pressure range (0 to 5) MPa at (298, 308, and 323) K and fitted with the Toth and multisite Langmuir models. Isosteric heats of adsorption were (12.8, 15.3, and 37.2) kJ/mol for nitrogen, methane, and carbon dioxide respectively, which indicate a very strong adsorption of carbon dioxide. The preferential adsorption capacity of CO_2 on zeolite 13X was much higher than for the other gases, indicating that zeolite 13X can be used for methane purification from natural gas or for carbon dioxide sequestration from flue gas.

Introduction

The use of natural gas as a fuel is advantageous from an environmental point of view and has become economically attractive. From the vantage of environmental protection, by use of natural gas as a vehicular fuel, reductions in CO, CO_2, and SO_2 are (97, 24, and 90) %, respectively, and the amount of lead discharged in exhaust gases is reduced to zero, and also it is cheaper than gasoline or diesel.

Currently, natural gas supplies one-fourth of the energy needed in the world's homes, businesses, vehicles, industries, and power plants, and the consumption of natural gas is expected to grow by 50% over the next 20 years.

Natural gas consists mainly of methane, typically (80 to 95) %, with variable amounts of C_{2+} hydrocarbons and often nitrogen and carbon dioxide as minor impurities. However, there exist many places where the carbon dioxide contamination exceeds 10%, like some sources in Germany (Central European Pannonian basin) or Australia (Cooper-Eromanga basin).[2] As an extreme of impurities present in a natural gas source, we can mention the effluent gas from a well undergoing CO_2 flooding that may contain (20 to 80) % CO_2.

To meet "pipeline-quality methane" the maximum amount of nitrogen and carbon dioxide cannot exceed 4% and 2%, respectively. The carbon dioxide reduction is also important to prevent equipment and pipeline corrosion.

Methane from coal beds, coalmines, and landfill gas is a rapidly growing source of natural gas; however, it often contains unacceptable levels of contaminants. As an example, a typical municipal or industrial landfill gas consists of approximately (40 to 60) % CO_2.[17]

Separation and purification of gas mixtures by adsorption has become a major unit operation in chemical and petrochemical industries. Pressure-swing adsorption technology has gained interest due to low energy requirements and low capital investment costs. Particularly in the case of the methane−carbon dioxide separation, many works have been published.[8,12] The group of Hirose[3] has used zeolite 13X and proposed a scheme of dual reflux to enrich

both methane and carbon dioxide starting from a mixture of methane and carbon dioxide diluted in nitrogen. Another important example is the Molecular Gate technology (Engelhard, USA) for both CO_2 and N_2 removal from natural gas streams using proprietary adsorbents.[5]

Once a selective adsorbent for carbon dioxide is found, an alternative application is carbon dioxide sequestration from flue gas. In this way, many works have used zeolite 13X to recover carbon dioxide from a binary mixture of CO_2 + N_2.[9] To design a pressure-swing adsorption (PSA) process, the basic information required is the adsorption equilibrium behavior of the pure components. In this work, we have gravimetrically measured high-pressure adsorption equilibrium of methane, carbon dioxide, and nitrogen on zeolite 13X at (298, 308, and 323) K and pressures ranging (0 to 5) MPa. The full set of data was fitted with the Toth model.
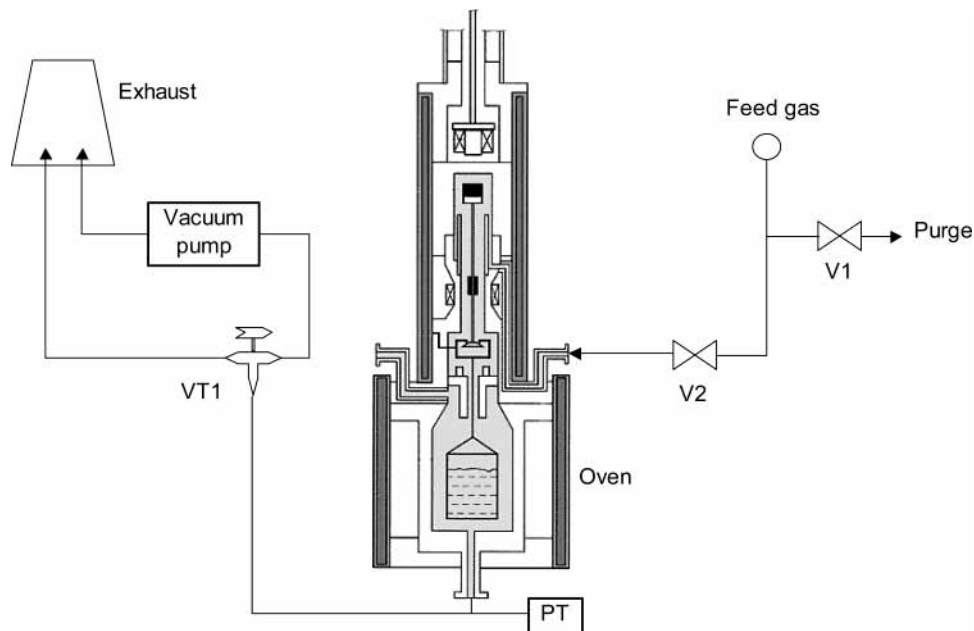
Experimental Section

Adsorption equilibrium of pure gases was performed in a magnetic suspension microbalance (Rubotherm, Germany) operated in closed system. A set-up of the equipment is shown in Figure 1. The sample of adsorbent is weighed and placed in a basket suspended by a permanent magnet through an electromagnet (magnetic suspension coupling). The cell in which the basket is housed is then closed, and a vacuum is applied. An analytical balance connected to the magnetic coupling receives the weight values measured inside the cell, and through an acquisition system, records the data in a computer. The accuracy of the microbalance is about $\pm 2 \times 10^{-8}$ kg. Two Lucas Schaevitz pressure transducers were used, one from (0 to 0.1) MPa with an accuracy $\pm 2 \times 10^{-5}$ MPa and another from (0 to 25) MPa with an accuracy $\pm 2.5 \times 10^{-3}$ MPa to acquire data at low and high pressures, respectively.

The activation of the sample was carried out under vacuum at 593 K overnight. The heating rate to reach this temperature was 2 K·min^{-1} with an accuracy of ± 0.01 K. Isotherms were measured at (298, 308, and 323) K in the range of (0 to 5) MPa. Adsorption and desorption measurements were performed, and all the isotherms were reversible.

The zeolite 13X extrudates were kindly provided by CECA (France). Some characteristic parameters of the

* To whom correspondence may be addressed. Phone: +351 22 508 1671. Fax: +351 22 508 1674. E-mail: arodrig@fe.up.pt.

Figure 1. Experimental set-up of the closed unit used for gravimetric measurements: V1 and V2, on−off valves; VT1, three-port valve; PT, pressure transducer; VP, vacuum pump.

Table 1. Experimental Data of Methane Adsorption Equilibrium on Zeolite 13X at 298 K to 308 K, and 323 K

T = 298 K		T = 308 K		T = 323 K	
P	q	P	q	P	q
MPa	mol·kg⁻¹	MPa	mol·kg⁻¹	MPa	mol·kg⁻¹
0.00000	0.000	0.00000	0.000	0.00000	0.000
0.00405	0.024	0.00525	0.022	0.00603	0.017
0.01203	0.089	0.01115	0.064	0.01215	0.052
0.01910	0.131	0.02040	0.109	0.02200	0.090
0.05515	0.326	0.04007	0.210	0.03302	0.140
0.125	0.712	0.08516	0.415	0.04612	0.196
0.165	0.877	0.135	0.623	0.05505	0.227
0.210	1.120	0.135	0.632	0.08010	0.312
0.306	1.474	0.190	0.823	0.115	0.432
0.345	1.617	0.280	1.133	0.165	0.590
0.425	1.830	0.310	1.232	0.240	0.731
0.631	2.357	0.350	1.360	0.340	1.009
0.819	2.726	0.445	1.618	0.340	1.009
1.070	3.060	0.585	1.931	0.400	1.193
1.180	3.260	0.585	1.932	0.510	1.423
1.410	3.530	0.695	2.154	0.505	1.395
1.720	3.834	0.780	2.342	0.635	1.653
1.890	3.991	0.875	2.466	0.780	1.929
2.175	4.198	1.110	2.792	0.865	2.077
2.610	4.506	1.480	3.201	0.955	2.211
2.985	4.750	1.700	3.409	1.185	2.545
3.365	4.987	1.790	3.480	1.495	2.890
3.560	5.103	2.170	3.781	1.695	3.067
3.745	5.191	2.530	4.038	1.860	3.169
3.745	5.191	2.535	4.034	2.425	3.577
4.260	5.469	2.840	4.236	2.570	3.670
4.725	5.719	3.640	4.702	3.015	3.933
		4.015	4.884	3.425	4.199
		4.490	5.127	3.425	4.200
		4.720	5.234	3.670	4.341
				4.180	4.585
				4.445	4.706
				4.745	4.830

Table 2. Experimental Data of Carbon Dioxide Adsorption Equilibrium on Zeolite 13X at 298 K, 308 K, and 323 K

T = 298 K		T = 308 K		T = 323 K	
P	q	P	q	P	q
MPa	mol·kg⁻¹	MPa	mol·kg⁻¹	MPa	mol·kg⁻¹
0.00000	0.000	0.00000	0.000	0.00000	0.000
0.00118	1.147	0.00126	0.825	0.00106	0.356
0.00610	2.249	0.00407	1.458	0.00214	0.529
0.02905	3.659	0.00905	2.060	0.00501	1.060
0.08610	4.500	0.01325	2.400	0.00907	1.430
0.160	5.060	0.02007	2.734	0.02423	2.090
0.310	5.580	0.04515	3.380	0.04220	2.490
0.525	6.040	0.09503	4.050	0.07503	2.900
1.015	6.520	0.160	4.490	0.145	3.400
1.015	6.500	0.220	4.740	0.270	3.915
1.445	6.920	0.280	4.960	0.390	4.100
1.935	6.960	0.370	5.167	0.545	4.329
2.280	7.090	0.485	5.315	0.705	4.532
2.660	7.220	0.570	5.399	0.850	4.740
3.200	7.372	0.700	5.586	1.010	4.820
		0.875	5.718	1.175	4.930
		0.875	5.718	1.455	5.200
		1.015	5.803	1.720	5.240
		1.200	5.942	2.125	5.430
		1.505	6.116	2.695	5.620
		1.830	6.291	3.395	5.762
		2.235	6.510		
		2.500	6.631		
		2.860	6.769		
		3.065	6.885		
		3.065	6.820		
		3.365	6.920		

(purities greater than (99.95, 99.998, and 99.995) %, respectively).

Data Handling and Treatment

As a first step in the description of the adsorption equilibrium, we must distinguish between absolute adsorption and excess adsorption. The difference between them is shown in eq 1[11]

$$q = q_{exc} + \frac{\rho_g V_{ads}}{m_s M} \tag{1}$$

adsorbent are summarized in Table 4. The average crystal size of the sample was obtained by scanning electron microscopy (SEM) and is presented in Figure 2. Many observations were performed indicating a very narrow crystal size distribution.

All gases used were provided by Air Liquide (Portugal): methane N35, carbon dioxide N48, and nitrogen N45

Table 3. Experimental Data of Nitrogen Adsorption Equilibrium on Zeolite 13X at 298 K, 308 K, and 323 K

T = 298 K		T = 308 K		T = 323 K	
P	q	P	q	P	q
MPa	mol·kg⁻¹	MPa	mol·kg⁻¹	MPa	mol·kg⁻¹

P MPa	q mol·kg⁻¹	P MPa	q mol·kg⁻¹	P MPa	q mol·kg⁻¹
0.00000	0.000	0.00000	0.000	0.00000	0.000
0.00613	0.024	0.00521	0.013	0.00903	0.015
0.01105	0.038	0.01217	0.029	0.01912	0.034
0.02511	0.082	0.02015	0.050	0.04006	0.074
0.0392	0.123	0.04503	0.108	0.05511	0.098
0.05003	0.156	0.05512	0.132	0.105	0.187
0.09002	0.264	0.08907	0.204	0.175	0.299
0.170	0.460	0.105	0.236	0.220	0.357
0.260	0.680	0.130	0.293	0.280	0.457
0.310	0.800	0.155	0.343	0.360	0.569
0.390	0.930	0.175	0.383	0.360	0.569
0.570	1.240	0.230	0.48	0.470	0.695
0.655	1.390	0.325	0.645	0.470	0.695
0.745	1.500	0.365	0.724	0.570	0.838
0.990	1.830	0.410	0.796	0.680	0.969
1.095	1.976	0.570	1.035	0.800	1.104
1.280	2.149	0.630	1.129	1.000	1.303
1.280	2.153	0.695	1.215	1.155	1.443
1.585	2.432	0.805	1.359	1.340	1.610
1.770	2.592	0.990	1.572	1.680	1.875
1.935	2.717	1.080	1.667	2.160	2.201
2.205	2.909	1.080	1.667	2.405	2.335
2.360	3.011	1.255	1.844	2.620	2.459
2.595	3.161	1.540	2.101	2.620	2.461
3.170	3.491	1.855	2.352	3.065	2.704
3.230	3.528	1.855	2.352	3.340	2.834
3.685	3.763	2.070	2.501	3.490	2.916
4.010	3.923	2.160	2.568	3.920	3.106
4.400	4.084	2.695	2.909	4.470	3.339
4.725	4.214	3.010	3.075	4.720	3.442
		3.295	3.260		
		3.710	3.451		
		4.015	3.588		
		4.465	3.785		
		4.705	3.888		

Table 4. Adsorbent Properties

| parameters	value
pellet particle density (kg·m⁻³)	1130
pellet diameter (m)	1.6×10^{-3}
crystal size (m)	7.0×10^{-7}
pellet porosity	0.54
macropore radius (m)	1.61×10^{-7}

where q is the absolute amount adsorbed, q_{exc} is the excess amount adsorbed, ρ_g is the density of the gas phase, and V_{ads} is the volume of the adsorbed phase. The second term corresponds to the "buoyancy" correction term. The main reason for this difference is that the volume of the adsorbed layer is not negligible, and gas density becomes closer to the density of the adsorbed layer especially at higher pressures where the density in the gas phase increases with pressure at a rate that is faster than that in the adsorbed phase, thus the last term of eq 1 cannot be neglected.[10]

The excess adsorption is obtained from adsorption measurements. On the other hand, the absolute adsorption cannot be obtained directly, and many approximate methods to calculate it from the excess adsorption were published.[4,10,11] In this work, we used a similar protocol reported by Dreisbach and co-workers.[4]

The microbalance signal Δm, measured when adsorption equilibrium is reached, is equal to

$$\Delta m = m - \rho_g(V_{ads} + V_s) \quad (2)$$

where m is the real mass of gas adsorbed and V_s is the volume of the solid adsorbent determined by helium.
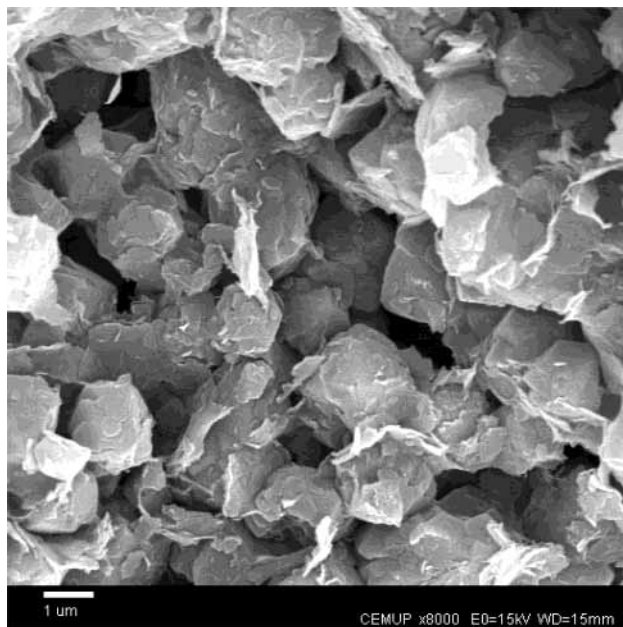
Figure 2. SEM image of the 13X zeolite (CECA).

The excess amount adsorbed is defined as

$$q_{exc} = \frac{\Delta m + V_s \rho_g}{m_s M} \quad (3)$$

where m_s is the mass of adsorbent and M is the molecular weight of gas. By doing so, we are assuming that helium penetrates in all the open pores of the sample without being adsorbed.[18]

The volume of the adsorbed phase is approximated by[4]

$$V_{ads} \cong \frac{m}{\rho_L} \quad (4)$$

where ρ_L is the density of the adsorbed phase, which is assumed to be equal to the density at the boiling point at 1 atm, selected as the reference-state conditions. Then, the total volume V is the sum of the adsorbed-phase volume, V_{ads}, and the volume of the adsorbent, V_s.

Replacing eq 4 into eq 2, we calculate the volume of the adsorbed phase, V_{ads} that is after used to calculate the total amount adsorbed by eq 1 using the excess amount adsorbed calculated by eq 3 straight from the experimental data.

The equilibrium data was fitted using the Toth model.[21] The equations corresponding to this model are

$$q_i = q_{mi} \frac{K_i P}{[1 + (K_i P)^{n_i}]^{1/n_i}} \quad (5)$$

$$K_i = K_i^0 \exp\left(-\frac{\Delta H_i}{RT}\right) \quad (6)$$

$$n_i = A_i + B_i T \quad (7)$$

where q_i and q_{mi} are the absolute amount adsorbed and the maximum amount adsorbed of component i, K_i^0 is the infinite adsorption constant, ΔH_i is the isosteric heat of adsorption at zero loading, n_i is the heterogeneity parameter, and A_i and B_i are the parameters relating the thermal variation of the heterogeneity coefficient. The isosteric heat of adsorption decreases with adsorbate loading for $n_i < 1$.[27]
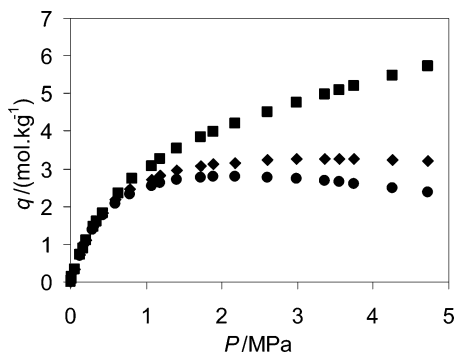
Figure 3. Methane adsorption equilibrium on zeolite 13X at 298 K. ■, absolute amount adsorbed, q; ◆, excess amount adsorbed, q_{exc}; ●, normalized microbalance signal ($M\Delta m/m_s$).

An alternative model to fit the pure component and binary data was the multisite Langmuir model. This model for homogeneous adsorbents derived by Nitta and co-workers[22] using statistical thermodynamic arguments proved its consistency for treatment of binary equilibrium data. A more general theory based on the mass-action law, where the Nitta model is a special case, has been recently proposed by Bhatia and Ding.[23] Neglecting adsorbate−adsorbate interactions, the model can be expressed as

$$\frac{q_i}{q_{mi}} = k_i P \left(1 - \frac{q_i}{q_{mi}} \right)^{a_i} \tag{8}$$

where a_i is the number of neighboring sites occupied by component i and k_i is the equilibrium constant from the Nitta model, which has an exponential dependence with temperature, also described by eq 6.

In this model, the isosteric heat of adsorption is not a function of adsorbate loading. The saturation capacity of each component is imposed by the thermodynamic constraint $a_i q_{mi}$ = constant.[24]

Fitting of the Toth and multisite Langmuir equations to experimental data was done with MATLAB 6.0 (The Mathworks, Inc). The best fitting parameters were found

Table 5. Fitting Parameters of the Toth Model

gas	q_{mi} mol·kg^{-1}	K_i^0 MPa^{-1}	$-\Delta H_i$ kJ·mol^{-1}	A_i	B_i K^{-1}
CH$_4$	9.842	2.50×10^{-3}	14.234	0.637	0
CO$_2$		6.86×10^{-3}	30.731	0.658	−0.0013
N$_2$		8.00×10^{-4}	14.935	0.661	0

Table 6. Fitting Parameters of the Multisite Langmuir Model

gas	q_{mi} mol·kg^{-1}	K_i^0 MPa^{-1}	$-\Delta H_i$ kJ·mol^{-1}	a_i
CH$_4$	28.871	4.34×10^{-4}	15.675	8.136
CO$_2$	17.901	3.20×10^{-8}	54.729	13.120
N$_2$	29.676	1.79×10^{-4}	15.716	7.917

by minimizing the objective function, square of residuals, SOR[27]

$$\text{SOR(\%)} = \sum_{T=1}^{3} \sum_{P=0}^{P\text{max}} \sum_{S=1}^{n} (q_{exp} - q_{calc})^2$$

where T_i are the three different temperatures used, P_{max} is the maximum pressure of each isotherm, and S is the number of points per isotherm per gas. The minimization routine used finds the minimum of the objective function using the Nelder−Mead Simplex Method of direct search. The error of the minimization function was settled to $|10^{-8}|$ (mol·kg^{-1})^2 between two consecutive iterations.

Results and Discussion

The first step in the experimental protocol is the helium adsorption measurements, done after the initial activation of the sample. Helium measurements were performed at ambient temperature (296 K) from vacuum up to 0.7 MPa. As the slope of the curve obtained was constant, we can assume that helium is not adsorbed[7] and from that value calculate the solid volume of the adsorbent.

An example of the use of the equations described above is shown in Figure 3, applying the protocol to the adsorption equilibrium isotherm of methane on zeolite 13X at 298 K where we show the microbalance signal (normalizing it
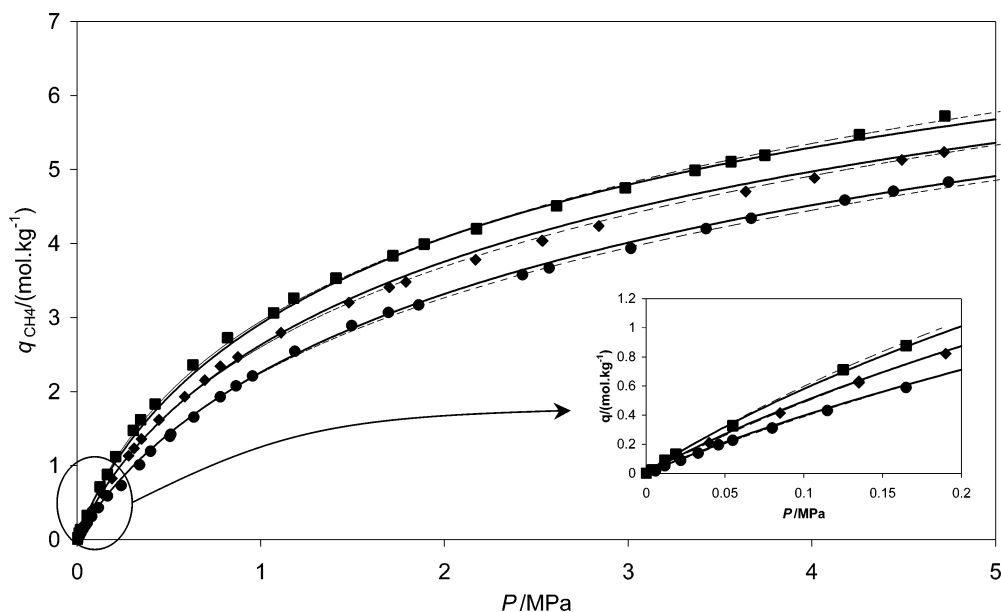
Figure 4. Methane adsorption equilibrium on zeolite 13X. ■, T = 298 K; ◆, T = 308 K; ●, T = 323 K; solid lines, Toth model; dotted lines, multisite Langmuir.
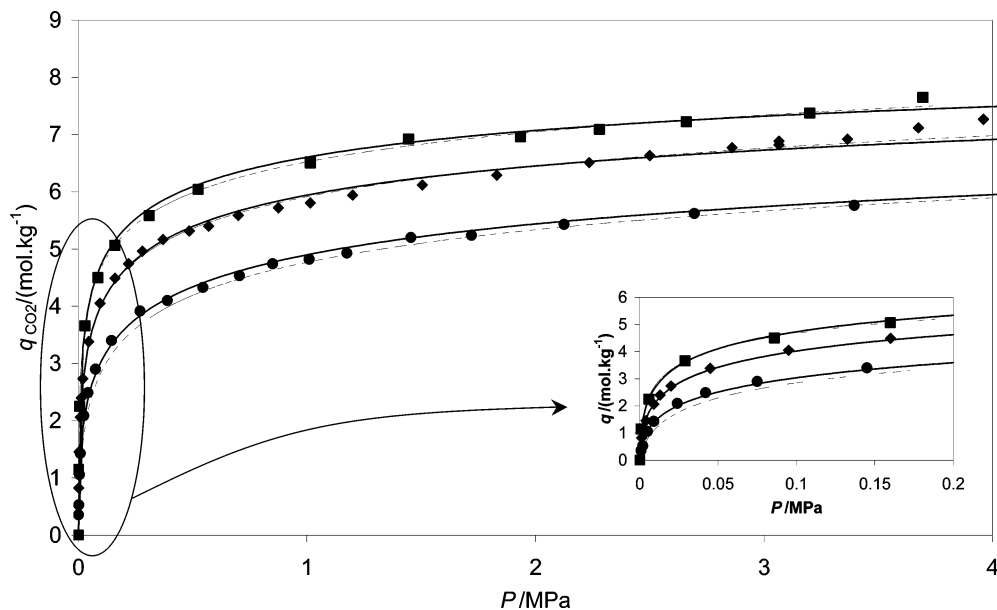
Figure 5. Carbon dioxide adsorption equilibrium on zeolite 13X. ■, T = 298 K; ◆, T = 308 K; ●, T = 323 K; solid lines, Toth model; dotted lines, multisite Langmuir.
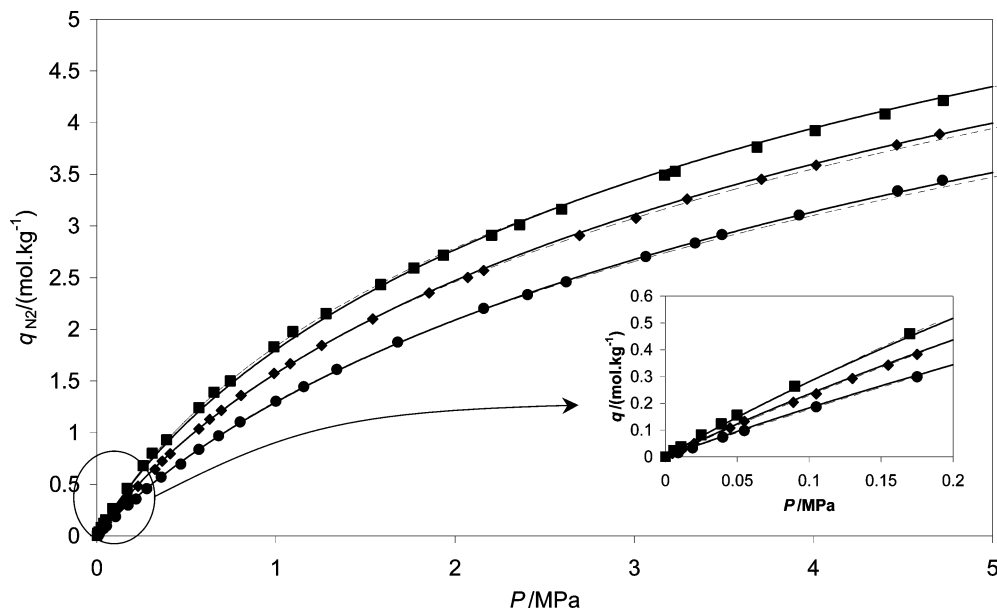
Figure 6. Nitrogen adsorption equilibrium on zeolite 13X. ■, T = 298 K; ◆, T = 308 K; ●, T = 323 K; solid lines, Toth model; dotted lines, multisite Langmuir.

to mmol/g, $= M\Delta m/m_s$), together with the excess amount adsorbed and the absolute amount adsorbed that has been calculated from eq 1.

The adsorption isotherms (absolute amount adsorbed per gram of adsorbent) of CH_4, CO_2, and N_2 on zeolite 13X at 298, 308, and 323 K are shown in Figures 4, 5, and 6. Solid lines in the figures represent the Toth isotherm fitting, while dotted lines represent the multisite Langmuir fitting. All the isotherms were completely reversible. At all pressures, carbon dioxide was the most adsorbed gas and nitrogen was the less adsorbed gas. The experimental data corrected are shown in Tables 1, 2, and 3.

As shown in Figures 4−6, the Toth model fits the data very well. The parameters of the fitting are reported in Table 5. The low-pressure region was amplified to see that the fitting of the Toth model is also good. A correct fitting of the low-pressure range is essential to describe well multicomponent data.[20] Written as in eqs 5−7, the Toth

model has five parameters, although the maximum amount adsorbed is the same for all gases. Also, the heterogeneity parameter is allowed to vary with temperature. Although this model is empirical, it has a very good flexibility to fit experimental data and it has a multicomponent extension that is easy to implement in PSA modeling.

A second analysis was performed using the multisite Langmuir model. This theoretical model offers a direct extension to multicomponent mixtures suitable for PSA modeling. The fitting using this model is also shown in Figures 3−5 (dotted lines) and the parameters employed are reported in Table 6. As the quality of the fitting is also very good, this model is preferred for adsorber design applications.

Adsorption equilibrium of methane has been compared with previous literature. The data presented compares very well with the low-pressure data in the linear range and up to 0.1 MPa.[13,25] At higher pressures, deviation of the
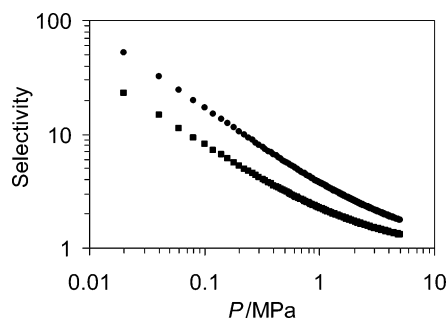
Figure 7. Ideal selectivity of carbon dioxide relative to methane and nitrogen: ■, CO_2/CH_4; ◆, CO_2/N_2.
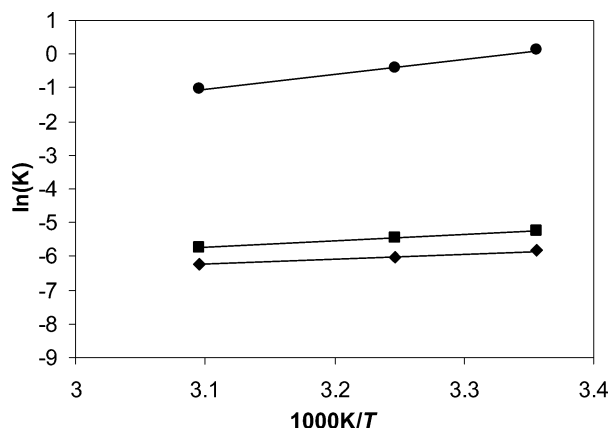
Figure 8. Arrhenius plot of the low-coverage isosteric heat of adsorption. ■, methane, $(-\Delta H_{CH_4}) = 15.294$ kJ·mol^{-1}; ◆, nitrogen, $(-\Delta H_{N_2}) = 12.764$ kJ·mol^{-1}; ●, carbon dioxide, $(-\Delta H_{CO_2}) = 37.222$ kJ·mol^{-1}.

data with previous literature is around 20%,[15] a difference that was also noted before when comparing methane adsorption equilibrium on zeolite 13X.[26] This difference at high pressures may be due to different assumptions used for the adsorbed phase density calculations used in the buoyancy correction.

The reported values of carbon dioxide are in agreement with previously published data, although the reported values of amount adsorbed are higher than all previous literature.[7,15,19] In the low-pressure range, the amount adsorbed compares very well with the data reported by Rege et al.[13]

When analyzing nitrogen adsorption equilibrium, the amount adsorbed is less than the one previously reported by Rege et al.[14] but compares very well with other data presented even in the high-pressure range.[1,19]

As can be seen from the equilibrium isotherms, the adsorbent is very selective to carbon dioxide. Preferential adsorption of CO_2 on zeolite 13X indicates that this material can be used for the separation of CO_2 from this gas mixture. The variation of the ideal selectivity (q_i/q_{CO_2}) of carbon dioxide relative to methane and nitrogen is shown in Figure 7.

The estimation of isosteric heat of adsorption was done with the low-pressure points (linear range of the isotherm), and the values are shown in Figure 8. Note that the value for CO_2 (37.2 kJ/mol) is very high when compared to the values of the other gases {(15.3 and 12.8) kJ/mol for CH_4 and N_2, respectively}. These values compare very well with previously reported values.[13] In the case of carbon dioxide, calorimetric studies report a decrease in the isosteric heat from (45 to 35) kJ/mol.[16] Because of the high affinity of carbon dioxide at low coverage, the estimation of the isosteric heat of adsorption may have large errors, explain-

ing the difference existing between this work and more straightforward methods such as calorimetric studies.

Conclusions

High-pressure adsorption equilibrium from gravimetric adsorption experiments for CH_4, CO_2, and N_2 were measured at (298, 308, and 323) K on zeolite 13X. The data were well fitted with the Toth and multisite Langmuir models. Isosteric heats of adsorption were (12.8, 15.3, and 37.2) kJ/mol for nitrogen, methane, and carbon dioxide, respectively, which indicate a very strong adsorption of carbon dioxide. The adsorbent is very selective to carbon dioxide, which makes it a very good candidate for methane purification from natural gas or for carbon dioxide sequestration from flue gas.

Literature Cited

(1) Beutekamp, S.; Harting, P. Experimental Determination and Analysis of High-Pressure Adsorption Data of Pure Gases and Gas Mixtures. *Adsorption* **2002**, *8*, 255−269.
(2) Krooss, B. M.; van Bergen, F.; Gensterblum, Y.; Siemons, N.; Pagnier, H. J. M.; David, P. High-Pressure Methane and Carbon Dioxide Adsorption on Dry and Moisture-Equilibrated Pennsylvanian Coals. *Int. J. Coal Geol.* **2002**, *51*, 69−92.
(3) Dong, F.; Kodama, A.; Goto, M.; Hirose, T. Simultaneous Separation of a Ternary Gas Mixture (CH_4-CO_2-N_2) by a Novel PSA Process. In *Fundamentals of Adsorption*; Le Van, D., Ed.; Kluwer Academic Publisher: Boston, 1998; pp 769−774.
(4) Dreisbach, F.; Staudt, R.; Keller, J. U. High-Pressure Adsorption Data of Methane, Nitrogen, Carbon Dioxide and their Binary and Ternary Mixtures on Activated Carbon. *Adsorption* **1999**, *5*, 215−227.
(5) Engelhard Corporation. Purification Technologies Brochure, 2001.
(6) Herbst A.; Harting P. Thermodynamic Description of Excess Isotherms in High-Pressure Adsorption of Methane, Argon and Nitrogen. *Adsorption* **2002**, *8*, 111−123.
(7) Hyun, S. H.; Danner, R. P. Equilibrium Adsorption of Ethane, Ethylene, Isobutane, Carbon Dioxide, and Their Binary Mixtures on 13X Molecular Sieves. *J. Chem. Eng. Data* **1982**, *27*, 196−200.
(8) Jee, J. G.; Kim, M. B.; Lee, C. H. Adsorption Characteristics of Hydrogen Mixtures in a Layered Bed: Binary, Ternary and Five-Component Mixtures. *Ind. Eng. Chem. Res.* **2001**, *40*, 868−878.
(9) Ko, D.; Siriwardane, R.; Biegler, L. T. Optimization of Pressure Swing Adsorption Process Using Zeolite 13X for CO_2 Sequestration. *Ind. Eng. Chem. Res.* **2003**, *42*, 339−348.
(10) Murata, K.; Kaneko, K. Nano-Range Interfacial Layer upon High-Pressure Adsorption of Supercritical Gases. *Chem. Phys. Lett.* **2000**, *321*, 342−348.
(11) Murata, K.; Miyawaki, J.; Kaneko, K. A Simple Determination Method of the Absolute Adsorbed Amount for High-Pressure Gas Adsorption. *Carbon* **2002**, *40*, 425−428.
(12) Olajossy, A.; Gawdzik, A.; Budner, Z.; Dula, J. Methane Separation From Coal Mine Methane Gas By Vacuum Pressure Swing Adsorption. *Trans. Ichem. E* **2003**, *81*, Part A, 474−482.
(13) Rege, S. U.; Yang, R. T.; Buzanowski, M. A. Sorbents for Air Prepurification in Air Separation. *Chem. Eng. Sci.* **2000**, *55*, 4827−4838.
(14) Rege, S. U.; Yang, R. T.; Kangyi, Q.; Buzanowski, M. A. Air-Prepurification by Pressure Swing Adsorption Using Single/Layered Beds. *Chem. Eng. Sci.* **2001**, *56*, 2745−2759.
(15) Rolniak, P. D.; Kobayashi, R. Adsorption of Methane and Several Mixtures of Methane and Carbon Dioxide at Elevated Pressures and Near Ambient Temperatures on 5A and 13X Molecular Sieves by Tracer Pertubation Chromatography. *AIChE J.* **1980**, *26* (4), 616−625.
(16) Siperstein, F. R.; Myers, A. L. Mixed-Gas Adsorption. *AIChE J.* **2001**, *47* (5), 1141−1159.
(17) Sircar, S. High Efficiency Separation of Methane and Carbon Dioxide Mixtures by Adsorption. *AIChE Symp. Ser.* **1988**, *84* (264), 70−72.
(18) Sircar, S. Measurement of Gibbsian Surface Excess. *AIChE J.* **2001**, *47*, 1169−1176.
(19) Siriwardane, R. V.; Shen, M.-S.; Fisher, E. P. Adsorption of CO_2 on Molecular Sieves and Activated Carbon. *Energy Fuels* **2001**, *15*, 279−284.
(20) Talu, O.: Needs, Status, Techniques and Problems with Binary Gas Adsorption Experiments, *Adv. Colloid Interface Sci.* **1998**, *76−77*, 227−269.
(21) Toth, J. State Equations of the Solid-Gas Interface Layers. *Acta Chim. Acad. Sci. Hung.* **1971**, *69*, 311−328.

(22) Nitta, T.; Shigetomi, T.; Kuro-Oka, M.; Katayama, T. An Adsorption Isotherm of Multisite Occupancy Model for Homogeneous Surface. *J. Chem. Eng. Jpn.* **1984**, *17*, 39−45.

(23) Bhatia, S. K.; Ding, L. P. Vacancy Solution Theory of Adsorption Revisited. *AIChE J.* **2001**, *47*, 2136−2138.

(24) Sircar, S. Influence of Adsorbate Size and Adsorbent Heterogeneity on IAST. *AIChE J.* **1995**, *41*, 1135−1145.

(25) Triebe, R. W.; Tezel, F. H.; Khulbe, K. C. Adsorption of Methane, Ethane and Ethylene on Molecular Sieve Zeolites. *Gas Sep. Purif.* **1996**, *10* (1), 81−84.

(26) Vermesse, J.; Vidal, D.; Malbrunot, P. Gas Adsorption on Zeolites at High-Pressure. *Langmuir* **1996**, *12*, 4190−4196.

(27) Do, D. D. *Adsorption Analysis: Equilibria and Kinetics*; Imperial College Press: London, 1998; p 66.